Bending rigidity and higher-order curvature terms for the hard-sphere fluid near a curved wall

Ignacio Urrutia*

Departamento de Física de la Materia Condensada, Centro Atómico Constituyentes, CNEA, Avenida Gral. Paz 1499, 1650 San Martin, Pcia. de Buenos Aires, Argentina

and CONICET, Avenida Rivadavia 1917, C1033AAJ Buenos Aires, Argentina

(Received 21 November 2013; published 19 March 2014)

In this work I derive analytic expressions for the curvature-dependent fluid-substrate surface tension of a hard-sphere fluid on a hard curved wall. In the first step, the curvature thermodynamic properties are found as truncated power series in the activity in terms of the exactly known second- and third-order cluster integrals of the hard-sphere fluid near spherical and cylindrical walls. These results are then expressed as packing fraction power series and transformed to different reference regions, which is equivalent to considering different positions of the dividing surface. Based on the truncated series it is shown that the bending rigidity of the system is non-null and that higher-order terms in the curvature also exist. In the second step, approximate analytic expressions for the surface tension, the Tolman length, the bending rigidity, and the Gaussian rigidity as functions of the packing fraction are found by considering the known terms of the series expansion complemented with a simple fitting approach. It is found that the obtained formulas accurately describe the curvature thermodynamic properties of the system; further, they are more accurate than any previously published expressions.

DOI: 10.1103/PhysRevE.89.032122 PACS number(s): 05.20.Jj, 05.70.Np, 64.70.qd, 64.70.pv

I. INTRODUCTION

The relation between the thermodynamic properties of a confined fluid and the shape of the vessel where it is confined has become a topic of current interest. Recently, inhomogeneous fluid cluster expansion was revisited and applied to a hard-sphere (HS) fluid near a hard planar wall [1]. Moreover, the HS system near spherical and cylindrical hard walls was studied, focusing on analysis of the curvature-dependent fluid-wall surface tension using both molecular dynamics (MD) and the density functional theory [2–4].

Studies of the *local* dependence of the surface tension or surface free energy on the curvature (for membranes, for two fluid-phases, and also for fluid/wall systems) rely on one of the two following expressions. The first one, derived by Helfrich [5], is

$$\gamma(J,K) = \gamma - \delta\gamma\, J + \frac{k}{2}J^2 + \bar{k}K + \cdots, \qquad (1)$$

where the truncation to order K is frequently assumed. The second expression, proposed by König *et al*. and based on the Hadwiger theorem [6], is

$$\gamma(J,K) = \gamma - \delta\gamma\, J + \bar{k}K. \qquad (2)$$

In Eqs. (1) and (2) $J = R_1^{-1} + R_2^{-1}$ is the total curvature, $K = R_1^{-1}R_2^{-1}$ is the Gaussian curvature, and R_1 and R_2 are the *local* principal radii of the surface. The fluid-wall surface tension (or surface free energy) for the case of a planar wall is indicated by γ, while the curvature coefficients are the Tolman's length δ, the bending rigidity k, and the Gaussian-curvature rigidity $\bar{k}$. Both Eq. (1) and Eq. (2) were successfully utilized to describe, on approximate grounds, the properties of interfaces. Furthermore, it was conjectured that Eq. (2) is complete for a HS fluid in contact with hard curved walls [7–9].

Analysis of the curvature-dependent surface tension is particularly simple in the context of constant curvature surfaces like cylindrical and spherical wall/fluid interfaces. In the last decade, different studies on HSs under these geometrical constraints were dedicated to evaluation of the bending rigidity, k. In the framework of the fundamental measure theory (FMT) of Rosenfeld, and based on the numerical analysis of the free energy, bending rigidity values compatible with $k = 0$ were found [7–9]. On the other hand, in the framework of a similar FMT an integral expression for k was derived, providing $k \neq 0$ and suggesting that Eq. (2) is not complete for this system. A second line of evidence supporting $k \neq 0$ results from the re-examination of MD results [3,4]. Unfortunately, the smallness of the maximum values obtained for k at a moderately low packing fraction η (<0.3)—$k(\eta = 0.2) = 0.000742$ using FMT and $k(\eta = 0.25) = 0.001 \pm 0.0008$ using MD, makes it necessary to take them with caution (here k is in units of k_BT, T being the temperature and k_B the Boltzmann constant). The main reason is that the method used to extract the curvature terms from MD depends on a fit which is very sensible in the adopted procedure. Second, FMT is an approximate theory that produces reliable results but not necessarily to this higher degree of accuracy.

In this work I study the higher-order curvature dependence of the surface tension for an HS fluid confined by spherical and cylindrical hard walls. The curvature-thermodynamic properties are obtained as power series in the activity and packing fraction and its coefficients to order 2 (for k and $\bar{k}$) or to order 3 [for $\delta\gamma$, $2k + \bar{k}$, and terms of order R^{-3} in Eq. (1)] are obtained exactly. An important finding presented here is that $k \neq 0$ on exact grounds and thus Eq. (2) is an approximated expression for the studied system. The effect that a change in the reference region (RR) produces on the system properties is revisited. The low-order series expansions of curvature-thermodynamic properties are also found by adopting a dividing surface typical of the scaled particle theory (SPT). Using the known terms in the series expansions complemented with the fitting of available data,

*urrutia@tandar.cnea.gov.ar

simple and accurate analytic expressions are presented for $\delta\gamma$ and $2k+\bar{k}$ and, for the first time, for k and $\bar{k}$. These expressions transformed to different RRs are verified by comparison with available data and it is concluded that they are the most accurate description of the analyzed properties developed at present.

II. EXPANSION IN THE ACTIVITY

The grand potential of a fluid of point particles confined in a region $\mathcal{A}$ by a hard wall (not necessarily a planar wall) can be expressed in power series form as

$$\beta\Omega = -\sum_{i\geqslant 1}\frac{\tau_i}{i!}z^i, \tag{3}$$

with τ_i the i-particle cluster integral of the fluid-in-$\mathcal{A}$ system, $\beta = 1/k_{\mathrm{B}}T$ its inverse temperature, and $z = \Lambda^{-3}\exp(-\beta\mu)$ its activity. Other magnitudes are the chemical potential μ, the de Broglie thermal length Λ, and $\beta\Omega = -\ln\Xi$, Ξ being the grand canonical partition function. For both spherical and cylindrical hard walls with a large enough radii R, the cluster integrals can be written as

$$\frac{\tau_i}{i!} = b_i V - a_i A + c_{i,1}\frac{A}{R} + c_{i,2}\frac{A}{R^2} + c_{i,3}\frac{A}{R^3} + \cdots, \tag{4}$$

where V is the volume of the system, A is its surface area, and R its radius. At a constant temperature the coefficients b_i, a_i, and $c_{i,j}$, with $j\geqslant 1$, are constant. Coefficients b_i and a_i are universal and correspond to the bulk cluster integrals [10] and to the planar-wall surface cluster integrals [11,12], respectively. On the other hand, $c_{i,j}$ may depend on the shape of the region where the fluid is confined. Naturally, if the wall is planar, $c_{i,j}=0$ for all j. Note that V, A, R, b_i, a_i, and $c_{i,j}$ refer to a given RR, $\mathcal{B}$, that follows the spherical/cylindrical symmetry of the one-body distribution function. Once $\mathcal{B}$ is fixed [through its radius $R=R(\mathcal{B})$] the description given in Eq. (4) is unique. Equations (3) and (4) suggest that

$$\Omega = -PV + \gamma A + C_1\frac{A}{R} + C_2\frac{A}{R^2} + C_3\frac{A}{R^3} + \cdots \tag{5}$$

or, equivalently,

$$\Omega = -PV + \gamma(R)A, \tag{6}$$

$$\gamma(R) = \gamma + C_1/R + C_2/R^2 + C_3/R^3 + \cdots, \tag{7}$$

with $P = \sum_{i\geqslant 1} b_i z^i$ the pressure of the bulk system (at the same z and T) and

$$\gamma = \sum_{i\geqslant 1} a_i z^i, \quad C_j = -\sum_{i\geqslant 1} c_{i,j} z^i, \tag{8}$$

$$\gamma(R) = \sum_{i\geqslant 1}\left(a_i - \sum_{j\geqslant 1} c_{i,j}R^{-j}\right)z^i. \tag{9}$$

Here, $\gamma(R)$ is the curvature-dependent fluid-wall surface tension and the functions C_j are thermodynamic curvature coefficients. The fluid-wall hard potential induces the formation of a surface with radius R_{d} where the one-body density distribution, $\rho(\mathbf{r})$, drops discontinuously to 0. The pressure on this zero-density surface, P_{o}, is given by the ideal-gas-like relation $P_{\mathrm{o}}/k_{\mathrm{B}}T = \rho(R_{\mathrm{d}})$, which is known as the wall or contact theorem. Given that $P_{\mathrm{o}} = -\frac{dR}{dV}\frac{\partial}{\partial R}\Omega$, one finds

$$P_{\mathrm{o}} = P + \gamma\frac{2}{R} + C_1\frac{1}{R^2} - C_3\frac{1}{R^4} + \cdots \quad \text{(sphere)}, \tag{10}$$

$$P_{\mathrm{o}} = P + \gamma\frac{1}{R} - C_2\frac{1}{R^3} - C_3\frac{2}{R^4} + \cdots \quad \text{(cylinder)}, \tag{11}$$

where $P = -\partial\Omega/\partial V$, $\gamma = \partial\Omega/\partial A$, $C_j = \partial\Omega/\partial(AR^{-j})$, and it was assumed that $R - R_{\mathrm{d}}$ is a constant length. The mean number of particles $N = -z\frac{\partial}{\partial z}\frac{\Omega}{kT} = \sum_{i\geqslant 1} i\frac{\tau_i}{i!}z^i$ can also be decomposed as Eqs. (5)–(9), resulting in expressions like $N = \rho V + \Gamma A + \Gamma^{(1)}A/R + \cdots$ and $N = \rho V + \Gamma(R)A$, where the density of the bulk system at the same z and T is

$$\rho = \sum_{i\geqslant 1} i b_i z^i, \tag{12}$$

Γ is the adsorption on a planar wall, $\Gamma^{(1)}$ is the first pure curvature adsorption, etc. In fact, the same method applies to higher-order derivatives too, for example, to the fluctuation in the number of particles $\langle N^2\rangle - N^2 = z\frac{\partial N}{\partial z} = \sum_{i\geqslant 1} i^2\frac{\tau_i}{i!}z^i$.

The Helfrich expansion given in Eq. (1) was originally derived for closed vesicles [5]. Vesicles are symmetric in the sense that the substances inside and outside are the same, therefore in this case the sign of J is fixed and can be chosen by convention. To apply Eq. (1) to the unsymmetrical system of a fluid in contact with a constant curvature hard wall, I adopt the usual convention, taking the curvature radius R_l as positive for the fluid outside of the spherical or cylindrical body. Therefore, in this work Eq. (1) reduces to

$$\gamma(R) = \gamma - 2\frac{\delta\gamma}{R} + \frac{2k+\bar{k}}{R^2} + \cdots \quad \text{(sphere)}, \tag{13}$$

$$\gamma(R) = \gamma - \frac{\delta\gamma}{R} + \frac{k}{2R^2} + \cdots \quad \text{(cylinder)}, \tag{14}$$

where higher-order terms like $C_{3(\mathrm{sph})}$ and $C_{3(\mathrm{cyl})}$ are included. These relations can be compared with Eq. (7) to obtain

$$\begin{aligned} \delta\gamma_{(\mathrm{sph})} &= -\tfrac{1}{2}C_{1(\mathrm{sph})}, \quad ck_{(\mathrm{sph})} = C_{2(\mathrm{sph})}, \\ \delta\gamma_{(\mathrm{cyl})} &= -C_{1(\mathrm{cyl})}, \quad k_{(\mathrm{cyl})} = 2C_{2(\mathrm{cyl})}, \end{aligned} \tag{15}$$

where the combined rigidity in short notation, $ck = 2k+\bar{k}$, has been introduced. Based on Helfrich's expression, none of the magnitudes γ, δ, k, or $\bar{k}$ depend on the geometry and thus (sph) and (cyl) labels should be unnecessary.

To prevent any question about the nonconvergence of the utilized virial-like power series I simply assume that $\Omega(z,R)$ is a well-behaved function of $z\in\mathbb{C}$ and $R\in\mathbb{C}$ at $z=0$ and $R=\infty$. This ensures that all the series from Eqs. (3) to (14) converge for real-positive values $z<z_{\mathrm{conv}}$ and $R>R_{\mathrm{conv}}$, z_{conv} and R_{conv} being the convergence radii of the $\beta\Omega(z,R)$ power series (note that both $z_{\mathrm{conv}}>0$ and $R_{\mathrm{conv}}>0$ exist but are unknown). Furthermore, the convergence readily extends to the series in powers of η given in Secs. III and IV. This well-behaved $\beta\Omega(z,R)$ is guaranteed for a diluted gas (low enough density and high enough temperature) and for a large enough R. On the contrary, the grand potential $\beta\Omega(z,R)$ becomes a nonanalytic function near the two-phase coexistence region both in bulk and under wetting-drying phenomena [13–15], which suggests that the above-utilized power series representations in z and R^{-1} cannot be used in these cases.

TABLE I. Bulk and surface (planar-wall) coefficients of the cluster integral τ_i up to $i = 5$. b_i and a_i have units of σ^3 and σ^4, respectively.

	$i = 2$	$i = 3$	$i = 4$	$i = 5$
b_i	$-2\pi/3$	$3\pi^2/4$	$-32.650\,6\ldots$	162.949 882 2 (5)
a_i	$-\pi/8$	$\frac{137}{560}\pi^2$	$-14.387\,1$ (6)	88.053 (10)

TABLE II. Curvature coefficients of the cluster integral τ_2 and τ_3. Known terms for spherical and cylindrical hard walls up to $j = 3$. $c_{i,j}$ has units of σ^{4+j}.

	$i = 2$ (sph)	$i = 3$ (sph)	$i = 2$ (cyl)
$c_{i,1}$	0	$-\frac{\pi}{768}(9\sqrt{3}+16\pi)$	0
$c_{i,2}$	$-\frac{\pi}{144}$	$\frac{781}{36288}\pi^2$	$-\frac{\pi}{384}$
$c_{i,3}$	0	$-\frac{\pi}{1280\sqrt{3}}$	0

III. THE HARD-SPHERE FLUID

For the fluid of an HS with hard repulsion distance σ (henceforth $\sigma = 1$, for simplicity) in contact with an HS wall, τ_2 and τ_3 were evaluated in Refs. [16] and [17]. In addition, for the case of a hard cylindrical wall the expression of τ_2 was found in Ref. [18]. Instead, the cluster integrals τ_i for $i > 3$ are only partially known from the values of b_i and a_i [19]. The coefficients b_i and a_i for $i = 2$, 3, 4, and 5 are listed in Table I.[1] Table II summarizes the known curvature coefficients of τ_i for spherical and cylindrical hard walls up to $j = 3$. These coefficients correspond to a choice of the RR, $\mathcal{B}$, that coincides with the available region for the center of each HS, $\mathcal{A}$, with $\rho(\mathbf{r} \notin \mathcal{A}) = 0$. Thus, under this density-based RR (d-RR), $R = R_\mathrm{d}$, which determines the position of the surface of tension, with $A = A_\mathrm{d} = 4\pi R_\mathrm{d}$ and $V = V_\mathrm{d} = 4\pi R_\mathrm{d}/3$. d-RR makes the evaluation of τ_i easy (e.g., in d-RR $\tau_1 = V$). Although using Eqs. (8) and (15) it is possible to explicitly write the curvature-thermodynamic properties as series expansion in powers of z, it is customary to show the results as functions of the packing fraction $\eta = \rho\sigma^3\pi/6$. Therefore, it is necessary to invert the series of Eq. (12) to find the series of $z(\eta)$ and then compose series to obtain the series expansion of each property in powers of η. Pressure and surface tension series reproduce the well-known virial series results, e.g., $\beta\gamma = -\frac{9\eta^2}{2\pi}(1 + \frac{149}{35}\eta) + O(\eta^3)$. For a spherical wall the series expansions of the curvature-thermodynamic properties give

$$\beta\,\delta\gamma_{(\mathrm{sph})} = -\frac{9}{64\pi^2}(9\sqrt{3}+16\pi)\eta^3 + O(\eta^4), \tag{16}$$

$$\beta\,ck_{(\mathrm{sph})} = \frac{\eta^2}{4\pi} - \frac{109\eta^3}{168\pi} + O(\eta^4), \tag{17}$$

and $\beta C_{3(\mathrm{sph})} = \frac{9\sqrt{3}}{160\pi^2}\eta^3 + O\left(\eta^4\right)$. On the other hand, for a cylindrical wall the series expansions are

$$\beta\,\delta\gamma_{(\mathrm{cyl})} = O(\eta^3), \quad \beta k_{(\mathrm{cyl})} = \frac{3\eta^2}{16\pi} + O(\eta^3), \tag{18}$$

and $\beta C_{3(\mathrm{cyl})} = O(\eta^3)$. Note that $\delta\gamma_{(\mathrm{sph})}$ and $\delta\gamma_{(\mathrm{cyl})}$ are consistent with the Helfrich's expansion at least up to the highest order for which both are known; i.e., $\delta\gamma_{(\mathrm{sph})} = \delta\gamma_{(\mathrm{cyl})} = \delta\gamma$ up to $O(\eta^3)$. Now, following Helfrich's expansion one finds

$$\beta\,\delta\gamma = -\frac{9}{64\pi^2}(9\sqrt{3}+16\pi)\eta^3 + O(\eta^4) \quad \text{(d-RR)}, \tag{19}$$

$$\beta\,ck = \frac{\eta^2}{4\pi} - \frac{109\eta^3}{168\pi} + O(\eta^4) \quad \text{(d-RR)}, \tag{20}$$

while the rigidity coefficients are

$$\beta k = \frac{3\eta^2}{16\pi} + O(\eta^3), \quad \beta\bar{k} = -\frac{\eta^2}{8\pi} + O(\eta^3) \quad \text{(d-RR)}. \tag{21}$$

Moreover, $c_{i,1(\mathrm{cyl})} = c_{i,1(\mathrm{sph})}/2$, showing that the unknown coefficient $c_{3,1(\mathrm{cyl})}$ (see Table II) is indeed $c_{3,1(\mathrm{cyl})} = -\frac{\pi}{384}(9\sqrt{3}+16\pi)$.

IV. DIFFERENT REFERENCE REGIONS

There are at least two RRs adopted in the literature. In the context of FMT it is usual refer the measures to the d-RR with radius $R = R_\mathrm{d}$, discussed in Sec. III [4]. On the opposite, in the SPT the focus is usually on the empty region (e-RR), which has a shifted radius of $R = R_\mathrm{e} = R_\mathrm{d} - 1/2$ (henceforth, magnitudes referring to the e-RR will be labeled with an e). Given that both e-RR and d-RR are widely utilized in the literature, it is interesting to transform the expressions found in the d-RR to obtain the series expansions in the e-RR.

No matter which reference is adopted, τ_i and Ω remain invariant because the system remains unmodified. To discuss a change of reference it is convenient to write Eq. (4) in matrix notation as

$$\tau_i/i! = (\mathbf{b}_i)_r\,\mathbf{M}_r, \tag{22}$$

where up to $O(A\,R^{-4})$ the vector of coefficients is $\mathbf{b}_i = (b_i, -a_i, c_{i,1}, c_{i,2}, c_{i,3})$ and the column matrix of measures is $\mathbf{M} = (V, A, AR^{-1}, AR^{-2}, AR^{-3})$. In fact, both $\mathbf{b}_i$ and $\mathbf{M}$ are relative to the adopted RR, and thus, I have introduced the generic label r to make it explicit. In Sec. III, the system is described on the basis of measures $\mathbf{M}_\mathrm{d} = (V_\mathrm{d}, A_\mathrm{d}, A_\mathrm{d}R_\mathrm{d}^{-1}, A_\mathrm{d}R_\mathrm{d}^{-2}, A_\mathrm{d}R_\mathrm{d}^{-3})$ and the corresponding vector of coefficients $(\mathbf{b}_i)_\mathrm{d}$. Measures taken with different RRs are related by a linear transformation, while the inverse transformation relates the corresponding coefficients. Here, the procedure is described for an RR with shifted radius $R = R_u = R_\mathrm{d} - u$ that corresponds to measures $\mathbf{M}_u = (V_u, A_u, A_uR_u^{-1}, A_uR_u^{-2}, A_uR_u^{-3})$, with the obvious definition for the volume and surface area of the sphere and the cylinder. In matrix form one finds

$$\tau_i/i! = (\mathbf{b}_i)_\mathrm{d}Y^{-1}Y\mathbf{M}_\mathrm{d} = (\mathbf{b}_i)_u\mathbf{M}_u, \tag{23}$$

[1]The coefficient b_4 is known exactly, its value being $-\pi^2(876\sqrt{2} + 94243\pi + 8262\,\mathrm{ArcCsc3})/90720$, while b_5 is evaluated using data from Ref. [19]. Both a_4 and a_5 are evaluated using a_2, a_3, and data taken from Ref. [1].

where $\mathbf{M}_u = Y\,\mathbf{M}_\mathrm{d}$ and $(\mathbf{b}_i)_u = (\mathbf{b}_i)_\mathrm{d}\,Y^{-1}$. To build the matrix Y, each measure in the u-RR frame is written as a linear function of the measures in the d-RR; for example, $V_u = V_\mathrm{d} + u\,A_\mathrm{d} - u^2 A_\mathrm{d} R^{-1} + \frac{u^3}{3} A_\mathrm{d} R^{-2}$. Therefore, $Y_{(\mathrm{sph})}$ and $Y_{(\mathrm{cyl})}$ are given by

$$\begin{pmatrix} 1 & u & -u^2 & u^3/3 & 0 \\ 0 & 1 & -2u & u^2 & 0 \\ 0 & 0 & 1 & -u & 0 \\ 0 & 0 & 0 & 1 & 0 \\ 0 & 0 & 0 & 0 & 1 \end{pmatrix} \quad \text{and}$$

$$\begin{pmatrix} 1 & u & -u^2/2 & 0 & 0 \\ 0 & 1 & -u & 0 & 0 \\ 0 & 0 & 1 & 0 & 0 \\ 0 & 0 & 0 & 1 & u \\ 0 & 0 & 0 & 0 & 1 \end{pmatrix}, \tag{24}$$

respectively [where terms of order $O(A_\mathrm{d} R^{-4})$ are depreciated]. The relation between $(\mathbf{b}_i)_u$ and $(\mathbf{b}_i)_\mathrm{d}$ directly implies the relation for the intensive properties: $(-P,\gamma,C_1,C_2,C_3)_u = (-P,\gamma,C_1,C_2,C_3)_\mathrm{d} Y^{-1}$. In particular, taking $u = 1/2$ it is possible to derive the properties in the e-RR for both the sphere and the cylinder cases. Thus, adopting the Helfrich expansion one finds, up to $O(\eta^4)$,

$$\beta\,\delta\gamma = -\frac{3\eta}{4\pi}\left[1 + \eta + \left(\frac{8}{35} + \frac{27\sqrt{3}}{16\pi}\right)\eta^2\right] \quad \text{(e-RR)}, \tag{25}$$

$$\beta\,ck = \frac{\eta}{4\pi}\left[1 + \frac{\eta}{2} + \left(\frac{81\sqrt{3}}{16\pi} - \frac{289}{105}\right)\eta^2\right] \quad \text{(e-RR)}, \tag{26}$$

while the rigidity constants up to $O(\eta^3)$ take the form

$$\beta k = \frac{3\eta^2}{16\pi}, \quad \beta\bar{k} = \frac{\eta}{4\pi}(1-\eta) \quad \text{(e-RR)}. \tag{27}$$

In addition, the next terms of higher order in R^{-1} are $\beta C_{3(\mathrm{sph})} = \frac{9\sqrt{3}\eta^3}{160\pi^2} + O(\eta^4)$ and $\beta C_{3(\mathrm{cyl})} = \frac{3\eta^2}{64\pi} + O(\eta^3)$. It is noteworthy that βk ($\beta C_{3(\mathrm{sph})}$) is independent of the chosen radius of the RR to any order in η because the fourth (fifth) column of $Y_{(\mathrm{cyl})}$ ($Y_{(\mathrm{sph})}$) is equal to the respective column of the identity matrix.

V. DEPENDENCE OF THE EQUATION OF STATE (EOS) ON η

Approximate expressions for γ, $\delta\gamma$, and ck as functions of η in the e-RR were obtained previously by Reiss *et al.* using the SPT [20] and, more recently, by Hansen-Goos and Roth [21], who combined an FMT approach known as WBII with Eq. (2). Both sets of approximate results were only utilized in the e-RR, while their accuracy under the adoption of a different RR was not verified. Therefore, in this section I transform SPT and WBII results to verify their accuracy in the d-RR. Yet, here I present a third set of expressions for the η dependence of γ, $\delta\gamma$, and ck based on the obtained first terms of their power series in η. Each of these three sets of functions, complemented with the bulk pressure EOS to build $(P,\gamma,\delta\gamma,ck)$, is compared with FMT and MD results to evaluate their performance and self-consistence in both the d-RR and the e-RR. Furthermore, using the same approach I found, for the first time, expressions for k and $\bar{k}$ as functions of η.

In the present proposal the functional dependence on η for each property will be obtained using the known exact low-order series terms and including one fitting parameter. To ensure that the thermodynamic properties are well described regardless of the adopted RR, the fitting is done in the framework of the d-RR and after transformed to the e-RR. In making the transformation between different RRs small inaccuracies in the EOSs may be magnified. Therefore, to transform consistently one must ensure that the pressure and the surface tension are accurately described. For $\beta P(\eta)$ one can adopt the very accurate Kolafa-Malijevsky low-density EOS [22]; however, I verified that the use of the Carnahan-Starling (CS) EOS instead of the Kolafa-Malijevsky low-density EOS introduces very small changes, and thus the simple and quasiexact CS, $\beta P(\eta)/\rho = (1+\eta+\eta^2-\eta^3)/(1-\eta)^3$, is utilized. On the other hand, there is not a sufficiently accurate EOS for the surface tension at present. Here, following the CS rational expression for P, I propose

$$\beta\gamma = -\frac{9\eta^2}{2\pi}\frac{1 + \frac{44}{35}\eta + \frac{1}{38}\eta^2 - 3(1-\eta)\eta^3}{(1-\eta)^3} \quad \text{(d-RR)}, \tag{28}$$

where the parameter is obtained by fitting and then transformed to the fraction $\frac{1}{38}$. Figure 1 shows a plot of the regularized difference between the fluid-wall surface tension γ taken from different sources and that given by Eq. (28), where the regularized version of a magnitude X (reg.X) is obtained by dividing X by the first term of its power series in η [e.g., reg.$\gamma = \gamma/(-9\eta^2/2\pi)$]. Plotted symbols are as follows: open and filled (green) circles represent MD results, taken from Refs. [2] and [3], respectively; (red) squares and (blue) diamonds correspond to density functional FMT results from Refs. [4] and [7], respectively; and points are Monte Carlo results. It is evident that Eq. (28) accurately describes the data, while other expressions for γ (η) (which are shown as different curves) deviate at $\eta \gtrsim 0.25$. For the curvature-thermodynamic properties I also utilized fitting functions that combine rational

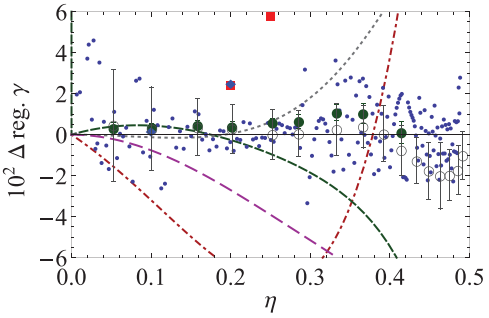

FIG. 1. (Color online) Difference among several results for the surface tension and the proposed analytic expression, Eq. (28) (in units of $k_\mathrm{B}T/\sigma^2$), using the d-RR. Plotted is the regularized magnitude γ (see text). Circles [open and filled (green)] are MD results from Refs. [2] and [3], (red) squares and (blue) diamonds correspond to FMT results from Refs. [7] and [4], and points are Monte Carlo results. The dot-dashed (red) line is the SPT result, the dashed (green) line is the WBII result, the long-dashed (magenta) line corresponds to the Henderson and Plischke [23] expression, and the dotted black line was obtained by Yang *et al.* [1].

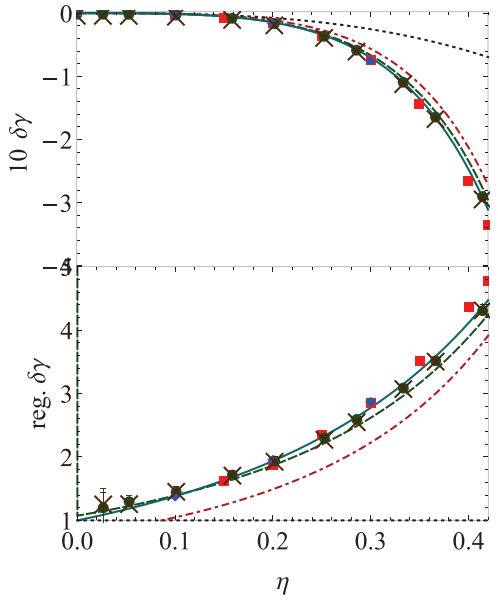

FIG. 2. (Color online) (a) The Tolman length times the surface tension in the d-RR (in units of $k_B T/\sigma$). (b) Regularized Tolman length. The (red) squares are FMT results of Bryk *et al.* [7], (blue) diamonds are FMT results of Blokhuis [4], and (green) circles and black crosses are MD results of Laird *et al.* [3]. The solid (light blue) line is the proposed expression, the dot-dashed (red) line is the SPT result, the dashed (green) line is the WBII result, and the dotted line is the exact series expansion truncated at the last known term.

and polynomial forms with one free parameter. They are

$$\beta\delta\gamma = -\left(\frac{9}{4\pi} + \frac{81\sqrt{3}}{64\pi^2}\right)\frac{\eta^3(1+1.2\eta)}{(1-\eta)^2} \quad \text{(d-RR)}, \qquad (29)$$

$$\beta ck = \frac{\eta^2}{4\pi}\frac{1-\frac{193\eta}{42}}{(1-\eta)^2} - 0.54\,\eta^4(1+3\eta) \quad \text{(d-RR)}, \qquad (30)$$

where 1.2 and −0.54 are fitting coefficients. In Fig. 2(a) the different symbols show the same behavior with increasing η, which is well described by WBII and fitted lines, while the SPT curve is slightly higher. Reg.$\delta\gamma$ is presented in Fig. 2(b). There, the FMT data are slightly separated from the MD data, showing some degree of discrepancy between them, and also, the SPT curve does not reproduce MD and FMT data with sufficient accuracy. On the other hand, the WBII curve correctly describes the data, the fitted curve being the most accurate. Given that the first non-null coefficient of $\delta\gamma$ as a power series in η is wrong for the SPT formula in the d-RR, its failure is not surprising. It is interesting to compare the FMT results found by Blokhuis and the WBII curve, based on slightly different FMT approaches. At $\eta = 0.3$ the difference between the two values of reg.$\delta\gamma$ is ∼0.15. This small difference is relevant because both methods are accurate in the sense that both involve negligible absolute errors and thus this disagreement is produced by minimal differences in the involved approximations. In this and subsequent figures I include results from a third-order polynomial fit in the reciprocal radius of the MD results [3] for the curvature-dependent surface tension of spherical and cylindrical hard walls. These results, plotted using crosses, were obtained by

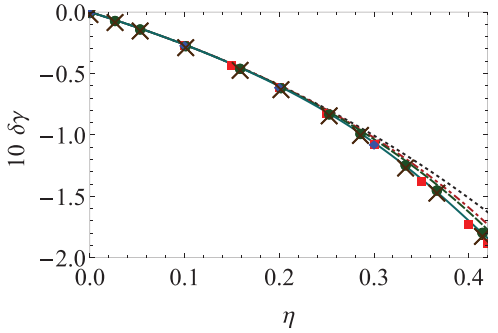

FIG. 3. (Color online) The Tolman length times the surface tension in the e-RR (in units of $k_B T/\sigma$). Lines and symbols are as described for Fig. 2.

first writing the $\gamma(R)$ data in each of the d-RR and e-RR and then fitting it. Figure 3 shows that Eq. (29) (found in the d-RR and then transformed to the e-RR) describes the behavior of the plotted symbols better than the other functional expressions and, also, that the series in η truncated to order η^3 follows the symbols in the e-RR much better than in the d-RR. The latter advantage of the e-RR with respect to the d-RR is confirmed in the subsequent figures. The results for the combined curvature term ck are presented in Figs. 4 and 5. In Figs. 4(a) and 4(b) it is clear that the best description of the behavior of MD and FMT data is given by Eq. (30), the WBII curve being slightly worse, while the worst of the three is the SPT curve. Figure 5 shows that in the e-RR the SPT and WBII produce nearly identical results which deviate from the symbols at large η. Instead, the order 3 series truncation given by Eq. (26) accurately describes the symbols. Again, one can verify that in the e-RR the best curve is provided by the present proposal. The difference between the Blokhuis

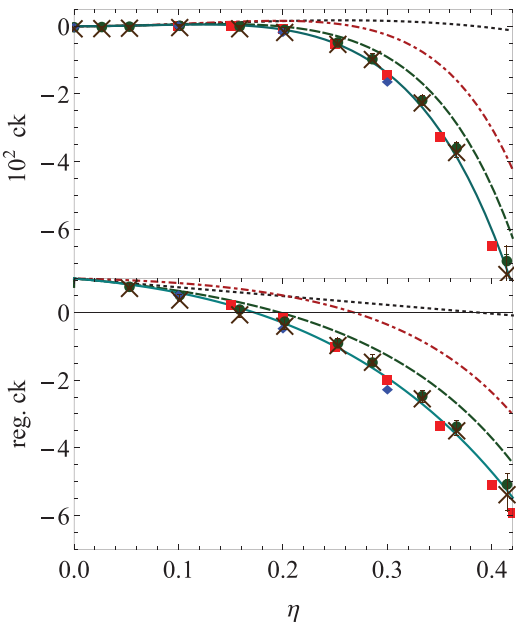

FIG. 4. (Color online) (a) Combined curvature rigidity $ck = 2k + \bar{k}$ in the d-RR (in units of $k_B T$). (b) The magnitude plotted in (a), but in its regularized form. Lines and symbols are as described for Fig. 2.

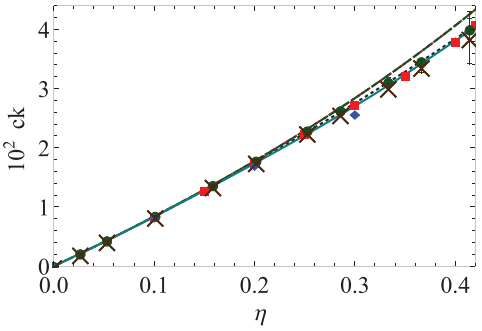

FIG. 5. (Color online) Combined curvature rigidity in the e-RR (in units of $k_B T$). Lines and symbols are as described for Fig. 2.

FMT results and the WBII curve in Figs. 4(a), 4(b), and 5 is apparent and grows with increasing packing fraction. On general grounds, the WBII describes the behavior of $\delta\gamma$ and ck in both the d-RR and the e-RR better than SPT, while the proposed expressions describes it still better. In addition, the observed discrepancies between FMT and WBII data suggest that one or both FMT-based results might not be reliable.

Expressions for the bending rigidity k and the Gaussian-curvature rigidity $\bar{k}$ have, to my best knowledge, never been presented in the literature. Now, for the bending rigidity the simple dependence

$$\beta k = \frac{3\eta^2}{16\pi}(1-3\eta) \quad (\mathrm{e}+\mathrm{d}-\mathrm{RR}) \tag{31}$$

is proposed, based on Eqs. (21) and (27) and the overall analysis of the data on regularized k. There the adjusted coefficient is -3. Figure 6 shows results for k in both the d-RR and the e-RR, which should be identical. In Fig. 6(a) the scale on the ordinate axes shows that k is of a very small magnitude. There, one can observe a large spread of the data. Moreover, the MD results show some degree of inconsistency in the values obtained adopting the d-RR (crosses) and the e-RR (circles with crosses), while the largest error bars cover the complete range of variation of k with η. All these features might indicate that the MD + fit procedure used to extract the k values is not completely reliable. In addition, the three FMT values suggest a nearly cubical behavior with a root at $\eta \sim 0.28$. The FMT approach is free of fitting uncertainties and has a high degree of self-consistence, which enables estimation of absolute errors that are very small, e.g., $\Delta k \simeq 10^{-8}$ for $\eta = 0.1$. However, a critical revision of the FMT adopted in Ref. [4] suggests that the values for k may be biased by the inaccuracy of the FMT itself at the high degree of detail shown in Fig. 6(a), where the diameter of the circles is 2×10^{-4} (in units of $k_B T$). This makes unclear the confidence that one should assign to the ability of these results to describe by themselves the subtle behavior of $k\,(\eta)$ for a *true* HS system. In particular, one source of inaccuracy in the adopted FMT is the use of the Percus-Yevick pressure EOS [24], which fails with increasing η. Based on Fig. 6(b) one notes that the FMT results suggest an overall linear behavior for the regularized form of k. Turning to the MD results, at low densities it is clear that neither set of data (which correspond to the d-RR and e-RR) points to the correct limiting value reg.$k \to 1$ with $\eta \to 0$ and, also, that the degree of inconsistency between them makes

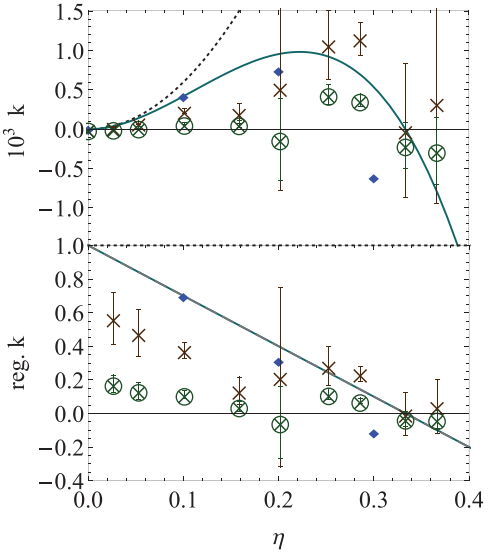

FIG. 6. (Color online) (a) Bending constant k for both the d-RR and the e-RR (in units of $k_B T$). (b) The magnitude plotted in (a), but in its regularized form. Diamonds (blue) are FMT results of Blokhuis [4]; crosses and circled crosses are MD results obtained by Laird *et al.*[3]. The solid (light-blue) line is the proposed expression, while the dotted black line is the exact series expansion truncated at the last known term.

them unreliable at low η. On the other hand, for $\eta \gtrsim 0.22$ the decrease in $k\,(\eta)$ and its nearly zero value is well established by the approximate coincidence of the MD and FMT results. Thus, I do not consider the MD results for $\eta \lesssim 0.22$, but I assume a simple linear behavior of the regularized k and make a crude estimate of the slope by considering the FMT value at the lower density ($\eta = 0.1$) and the MD results for

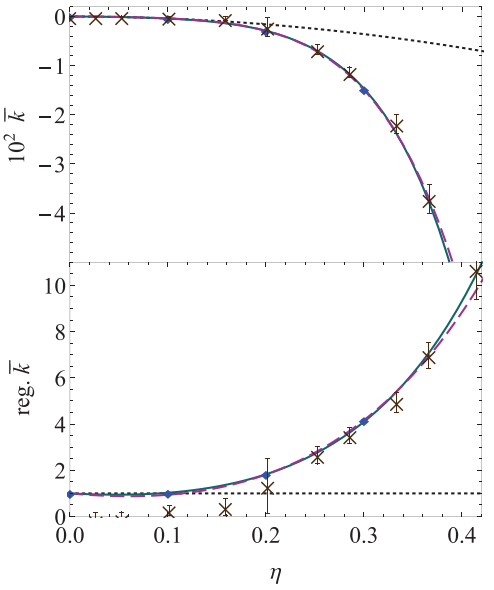

FIG. 7. (Color online) (a) Bending constant $\bar{k}$ (in units of $k_B T$) in the framework of the d-RR. (b) The magnitude plotted in (a), but in its regularized form. Lines and symbols are as described for Fig. 6, except for the dashed (magenta) line, obtained from Eqs. (30) and (31) as $ck - 2k$.

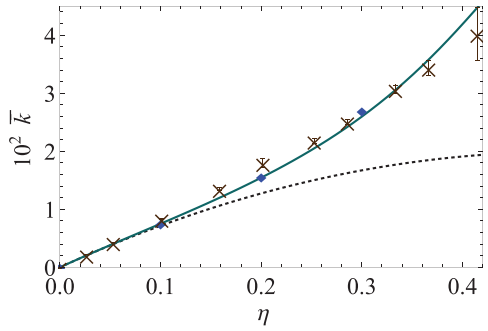

FIG. 8. (Color online) Bending constant $\bar{k}$ (in units of $k_B T$) in the framework of the e-RR. Lines and symbols are as described in Fig. 6.

$\eta \gtrsim 0.22$. Based on this analysis, I found a slope of -3, which corresponds to Eq. (31) and is plotted in the figure. For the Gaussian-curvature rigidity I propose

$$\beta\bar{k} = -\frac{\eta^2}{8\pi}\frac{1 - 4.2\,(1-6\eta)\,\eta}{(1-\eta)^2} \quad \text{(d-RR)}, \tag{32}$$

where -4.2 was found by fitting. In Fig. 7(a) it is plotted $\bar{k}$ in d-RR. There, one can verify the accurate fitting of Eq. (32) to the MD and FMT data, as well as the consistence between the fitted $\bar{k}$ and that found from Eqs. (30) and (31) as $ck - 2k$. In Fig. 7(b) it is apparent that for $\eta \lesssim 0.2$, the MD data do not show the correct behavior because they do not go to unity when $\eta \to 0$; this inconsistency is clearly related to that found in Fig. 6(b) and makes the MD data for this range of η unreliable. Therefore, Eq. (32) is obtained by fitting the three FMT points and those of MD for $\eta \gtrsim 0.2$. The consistency of the approach is verified by the coincidence with the alternative route to $\bar{k}$ plotted by the dashed line. The expression in Eq. (32) transformed to the e-RR is plotted in Fig. 8. Again, the curve fits the data very well, which validates the obtained description.

VI. FINAL REMARKS

In this work the series expansions for the Tolman length and for the combination of curvature terms $2k + \bar{k}$ were evaluated up to order 3 in the packing fraction. Furthermore, the dependences of both the bending rigidity and the rigidity constant associated with the Gaussian curvature were found up to order 2 in the packing fraction. All these findings are absolute in the sense that they do not imply the assumption of a nonexact EOS, are based on the exact value of the coefficients, and can be readily transformed on exact grounds to any RR. Moreover, the functional dependence of these curvature-thermodynamic properties on the packing fraction away from $\eta \gtrsim 0$ was established on the basis of an approximate and accurate fitting procedure.

Based on the truncated power series in the packing fraction, definitive evidence is presented showing that for an HS fluid in contact with hard-curved walls $k \neq 0$ and, then, that Eq. (2) proposed by König *et al.* [8,9] based on the Hadwiger theorem [6,25] is not a complete expression for $\gamma\,(J,K)$, at least for the studied system. The same conclusion extends to the complete morphological thermodynamic approach, which may be considered a good approximate theory, but not an exact one. This result is in good agreement with that found previously using FMT [4]. However, it must be remarked that the use of free energy density functional theories like FMT for the evaluation of small and sensible quantities should be done with caution. FMT is an approximate theory for inhomogeneous fluids, and thus, the boundaries of reliability of the involved approximations are *a priori* unclear. Particularly, its capability to describe the subtle behavior of k and its degree of confidence should be studied further.

Moreover, it is shown that the order $O(A\,R^{-4})$ terms in $\gamma\,(R)$ are non-null and, thus, that the truncation up to order J^2 and K of the Helfrich expansion is also incomplete and does not enable accurate description of the known properties of the HS inhomogeneous system. Notably, the expressions for $\tau_{2(\mathrm{cyl})}\,(R)$ and $\tau_{3(\mathrm{sph})}\,(R)$, which in this work were truncated to order A/R^3, enable us to readily extend the results to any order in powers of R^{-1}, showing that the Helfrich expression is also *approximate* if one truncates it to any finite order in R^{-1}. The accuracy of the obtained analytic expressions for γ, $\delta\gamma$, ck, k, and $\bar{k}$ based on data fitting is largely restricted by the small discrepancies between the different theoretical methods utilized to obtain the data. In this sense, the development of a direct Monte Carlo–based method to evaluate the curvature-thermodynamic properties might be necessary to improve the reliability and accuracy of numerical results.

ACKNOWLEDGMENTS

I am grateful to Jung Ho Yang and David A. Kofke for kindly providing me with the surface tension Monte Carlo data published in Ref. [1] and to Gabriela Castelletti and Claudio Pastorino for helpful discussions and comments. This work was supported by CONICET PIP-0546/10, UBACyT 20020100200156, and ANPCyT PICT-2011-1887.

[1] J. H. Yang, A. J. Schultz, J. R. Errington, and D. A. Kofke, J. Chem. Phys. **138**, 134706 (2013).
[2] B. B. Laird and R. L. Davidchack, J. Chem. Phys. **132**, 204101 (2010).
[3] B. B. Laird, A. Hunter, and R. L. Davidchack, Phys. Rev. E **86**, 060602 (2012).
[4] E. M. Blokhuis, Phys. Rev. E **87**, 022401 (2013).
[5] W. Helfrich, Z. Naturforsch. C **28**, 693 (1973).
[6] H. Hadwiger, *Vorlesungen über Inhalt, Oberfläche und Isoperimetrie* (Springer, Basel, 1957).
[7] P. Bryk, R. Roth, K. R. Mecke, and S. Dietrich, Phys. Rev. E **68**, 031602 (2003).
[8] P. M. König, R. Roth, and K. R. Mecke, Phys. Rev. Lett. **93**, 160601 (2004).

[9] P. M. König, P. Bryk, K. R. Mecke, and R. Roth, Europhys. Lett. **69**, 832 (2005).
[10] T. L. Hill, *Statistical Mechanics* (Dover, New York, 1956).
[11] A. Bellemans, Physica **28**, 493 (1962).
[12] S. Sokołowski and J. Stecki, Acta Phys. Pol. **55**, 611 (1979).
[13] R. Evans, R. Roth, and P. Bryk, Europhys. Lett. **62**, 815 (2003).
[14] R. Evans, J. R. Henderson, and R. Roth, J. Chem. Phys. **121**, 12074 (2004).
[15] M. C. Stewart and R. Evans, Phys. Rev. E **71**, 011602 (2005).
[16] I. Urrutia, J. Stat. Phys. **131**, 597 (2008).
[17] I. Urrutia, J. Chem. Phys. **135**, 024511 (2011); Erratum, **135**, 099903 (2011).
[18] I. Urrutia, J. Chem. Phys. **133**, 104503 (2010).
[19] N. Clisby and B. M. McCoy, J. Stat. Phys. **122**, 15 (2006).
[20] H. Reiss, H. L. Frisch, E. Helfand, and J. L. Lebowitz, J. Chem. Phys. **32**, 119 (1960).
[21] H. Hansen-Goos and R. Roth, J. Phys.: Condens. Matter **18**, 8413 (2006).
[22] J. Kolafa, S. Labík, and A. Malijevský, Phys. Chem. Chem. Phys. **6**, 2335 (2004).
[23] D. Henderson and M. Plischke, Proc. Roy. Soc. London A: Math. Phys. Sci. **410**, 409 (1987).
[24] M. S. Wertheim, Phys. Rev. Lett. **10**, 321 (1963).
[25] K. R. Mecke, Int. J. Mod. Phys. B **12**, 861 (1998).